INTERNATIONAL JOURNAL OF INTEGRATED ENGINEERING
ISSN: 2229-838X e-ISSN: 2600-7916

IJIE

Vol. 16 No. 4 (2024) 8-15
https://publisher.uthm.edu.my/ojs/index.php/ijie

Quantifying Desiccation Cracks for Expansive Soil Using Machine Learning Technique in Image Processing

Hui Yean Ling[1], See Hung Lau[1,2]*, Siaw Yah Chong[1,2], Min Lee Lee[3], Yasuo Tanaka[1,2]

[1] *Department of Civil Engineering, Lee Kong Chia n Faculty of Engineering and Science Universiti Tunku Abdul Rahman, 43000 Kajang, Selangor, MALAYSIA*

[2] *Centre of Disaster Risk Reduction Universiti Tunku Abdul Rahman, 43000 Kajang, Selangor, MALAYSIA*

[3] *Department of Civil Engineering, Faculty of Science & Engineering University of Nottingham Malaysia, 43500 Semenyih, Selangor, MALAYSIA*

*Corresponding Author: laush@utar.edu.my
DOI: https://doi.org/10.30880/ijie.2024.16.04.002

Article Info

Received: 9 January 2024
Accepted: 12 June 2024
Available online: 12 August 2024

Keywords

Global environmental issues, desiccation crack, machine learning, image processing technique, crack quantification, kaolinite

Abstract

The formation of desiccation cracks has detrimental effects on the hydraulic conductivity that affects the overall mechanical strength of expansive soil. Qualitative analysis on the desiccation cracking behaviour of expansive soil provided understanding of the subject based on various concepts and theories, while quantitative analysis aided these studies through numerical supports. In this study, a machine learning technique in image processing is developed to evaluate the surface crack ratio of expansive soil. The desiccation cracking tests were conducted on highly plastic kaolinite slurry samples with plasticity index of 29.1%. Slurry-saturated specimens with thickness of 10 mm were prepared. The specimens were subjected to cyclic drying-wetting conditions. The images are acquired through a digital camera (12 MP) at constant distance to monitor the desiccation cracks. The images are then pre-processed using OpenCV before crack feature extraction. In this study, a total of 54 desiccation crack images were processed, along with 8 images from trial test to train the model. The processed images are used to quantify the desiccation cracks by evaluating surface crack ratio and average crack width. It was identified that the accuracy of the model for the quantification of surface crack ratio and average crack width were 97.24% and 93.85% respectively with average processing time of 1.51s per image. The results show that the model was able to achieve high accuracy with sufficient efficiency in determining important parameters used for crack characterization.

1. Introduction

Desiccation cracking also known as shrinkage cracking on soil occurs due to moisture lost in the soil. Volumetric shrinkage causes the buildup of tensile stress from matric suction during desiccation process, and crack is generated when this stress exceeds the tensile strength of soil [1]. The tensile stress developed tends to degrade the hydraulic and mechanical properties of soil [2]-[4]. Crack formation can affect the performance and application of clay in various sectors including geotechnical, geo-environmental, and agricultural fields.

Climate change imposed substantial influence on the consistency of the recurring drying and wetting cycles, bringing higher frequency of extreme weather with dryer dry season and wetter wet season [5], making the

recognition of desiccation cracks crucial. Quantitative analysis is becoming more important in desiccation cracking studies as the crack patterns are linked to the historical load and might affect its future functionality. Numerous research has been conducted to analyse and describe soil cracks based on manual approach (e.g., wired probe [6], polythene sheets [7], cement slurry [8], and dye [9]), and non-intrusive approach (e.g., image analysis [9], [10]). Some manual methods that include low capital and readily available equipment can disturb the original crack patterns, resulting in measurement with low accuracy [11]. This led to the advancement of the quantitative analysis approach from manual to image analysis techniques, which focused on extracting useful information from crack patterns such as crack width, length, and shape through collected visual data [12]. For the analysis, majority of existing investigations on digital image processing of desiccation cracking patterns rely on commercial graphics software or open-source image processing program, which are not suitable for desiccation cracks studies and are incapable of providing comprehensive quantitative analysis of crack patterns [1], [10], [12], [14]. Therefore, the incorporation of machine learning techniques in image processing is the new method to provide better crack detection performance.

Machine learning-based image processing involved pre-processing steps and noise removal in conventional image processing techniques to prepare the images for crack detection by a trained machine learning model [15]. Xu et al. [16] carried out semantic segmentation in clayey soil cracking network detection using U-Net CNN algorithm. Parente et al. [17] presented a simplified machine learning-based crack monitoring method through open sources software that successfully detects cracks with single-image training. Han et al. [18] proposed Mask R-CNN structure for the detection and instance segmentation of clayey soil desiccation cracks. As the use of machine learning techniques in desiccation crack recognition is still in its premature phase, further validation is essential in assessing its reliability in crack quantification analysis.

In this study, laboratory experiments on desiccation tests were conducted on kaolinite slurry to investigate its desiccation cracking behaviour under repeated wetting and drying cycles. This study investigated the viability and efficacy of machine learning for estimating the desiccation cracking of expansive soil. Laboratory-scale image collection was conducted through the use of a digital camera. The acquired images were then pre-processed and processed with image processing model architected based on machine learning algorithm. Quantification of desiccation cracks through feature extraction was based on defined parameters such as surface crack ratio and average crack width. The proposed technique proved to forecast the fracture intensity factor with satisfactory precision.

2. Methods

2.1 Materials

The expansive soil used in this investigation was kaolin clay. The clay had a particle size range of 2.0 μm to 3.0 μm. Soil classification tests were conducted prior to sample preparation. The chemical composition of the kaolin clay (through XRF test method) is shown in Table 1, along with the properties obtained from soil tests.

Table 1 *Chemical composition and soil properties of kaolin clay*

Chemical Components	Composition
Aluminum (Al_2O_3)	32.0 – 38.0%
Silica (SiO_2)	47.0 – 53.0%
Loss on Ignition @ 1025°C	11.0 – 14.0%
Soil Properties	
Liquid Limit (LL)	66.0%
Plastic Limit (PL)	36.9%
Plasticity Index (PI)	29.1%
BSCS Classification	MH (highly plastic silt)

2.2 Sample Preparation

The specimens were prepared at targeted moisture content of about 120%. The mixture was stirred until a homogenous slurry state was reached. The slurry was then sealed and left for 24 hours at room temperature. This is essential to ensure that the moisture is uniformly distributed in the soil [1]. The samples were then prepared by pouring the slurry into 120 mm (D) x 20 mm (H) glass Petri dishes until desired height was achieved. Vibration was applied to remove the entrapped air. The specimens were subjected to two drying methods i.e., oven drying and 45°C drying approach.

Int. Journal of Integrated Engineering Vol. 16 No. 4 (2024) p. 8-15

2.3 Desiccation Tests

The prepared specimens were subjected to 4 wetting and drying cycles under 2 drying approaches. The first drying method was oven drying which provided 105°C drying temperature and 0% relative humidity. The second drying approach was drying under controlled temperature and relative humidity (RH) of 45 ± 2°C and 40 ± 5% respectively. These controlled drying conditions were achieved using a humidity chamber and oven bulbs as shown in Fig. 1. Distilled water was added for the wetting phase. The volume of water added was based on the mass of moisture lost in the preceding drying path to achieve the initial water content. The re-hydrated specimens were left to stand for 24 hours (sealed) before the commencement of the subsequent drying cycle. A digital camera with 12 MP resolution was used to capture the surface cracking patterns throughout the test at varying time intervals. The acquired images were then fed to an image processing model for crack quantification.

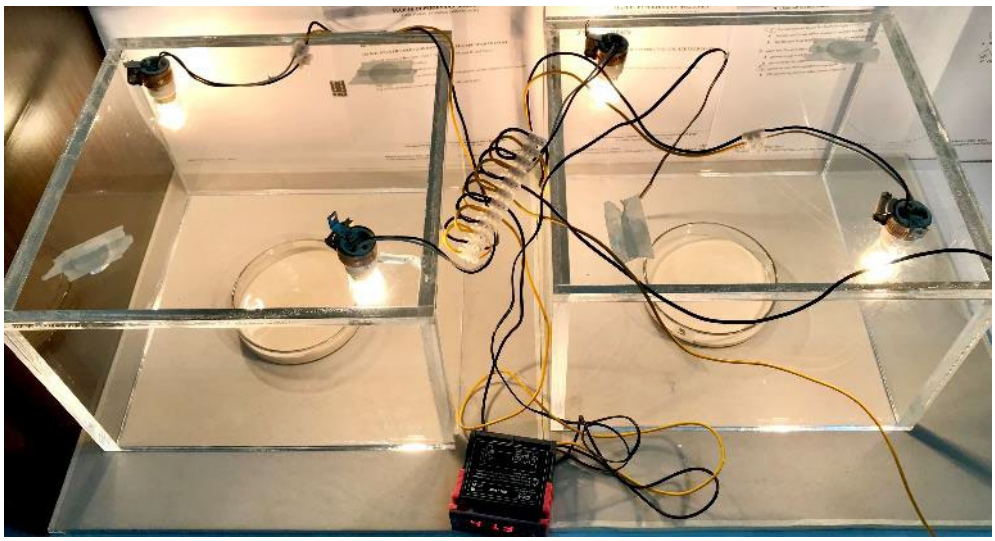

Fig. 1 *Second drying approach set up with humidity chamber*

2.4 Image Processing

The image processing model was architected with Python as the programming language and OpenCV as image processing application. In this model, OpenCV was imported to Python for image processing functions. The acquired images were cropped to specimen size to remove unnecessary information contained in the outer region of the sample, then these raw RGB images were subjected to pre-processing, processing, and feature extraction to achieve crack quantification and the image undergo pre-processing steps including grey-scaled using grey scaling function (minimized processing needs) and noise filtering by median filter (remove noise). In the processing stage, the image was subjected to: (i) Sobel operator as edge detection algorithm that detects discontinuities and information's edge so that the crack edges can be emphasized in the output image; (ii) thresholding to separate useful and unnecessary pixels, and convert useful ones (crack) into white pixel while unnecessary ones into black pixel; (iii) morphological closure to make fracture line display more visible; (iv) contour area function to reduce noise in the processed binary image; (v) filling method through dilation and erosion steps that converted the black pixels enclosed within white pixels to white pixels. At last, circle function and bitwise function were applied to draw a circle that eliminates the mould of the soil so the image was readied for feature extraction. The sample image after each process is shown in Fig. 2.

2.5 Information Extraction

The desiccation cracks were quantified by evaluating surface crack ratio and average crack width. Surface crack ratio (SCR) was calculated by dividing the crack pixel by background pixel where the crack pixel was determined using contour area function.

$$\text{Surface Crack Ratio, \%} = \frac{P_W}{P_T} \tag{1}$$

where P_W is the white pixel which represents the crack pixel and P_T is the total pixel in the image (background pixel).

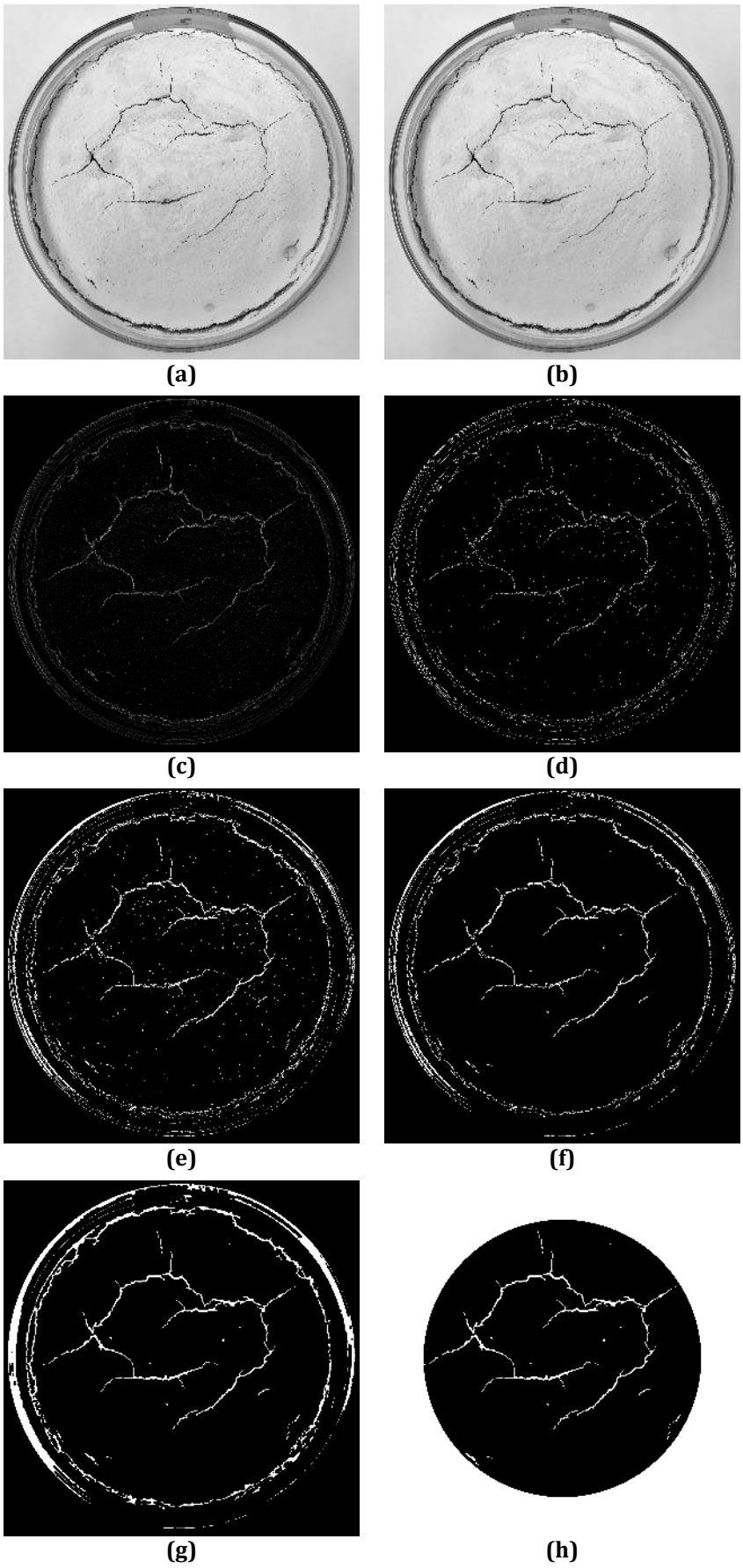

Fig. 2 *Stages in Images Processing model (a) Gray scaling; (b) Median filtering; (c) Sobel operator; (d) Thresholding; (e) Morphological closure; (f) Contour area function; (g) Filling; (h) Circle and bitwise*

Int. Journal of Integrated Engineering Vol. 16 No. 4 (2024) p. 8-15

To evaluate average crack width, skeletonization was applied to the binary image to convert the crack lines to single pixel width. Average crack width was then computed by dividing crack pixel (P_C) by skeletonized crack pixel ($P_{C,S}$) as shown in the equation below.

$$\text{Average Crack Width, mm} = \frac{P_C}{P_{C,S}} \tag{2}$$

The efficiency and capability of the proposed model were assessed through its processing time and accuracy. The average processing time for each image was estimated by dividing the total time taken to process the total number of images by the total number of images processed. The accuracy of the model was assessed by averaging the results from the images with identical crack patterns but acquired under different photography skills. The equation for accuracy assessment is shown below.

$$\text{Accuracy Assessment for Each Dataset} = 100\% - \left(\frac{x_i - \frac{\sum x}{n}}{\frac{\sum x}{n}} \times 100\% \right) \tag{3}$$

where x_i is the current data of the image to be tested, $\sum x$ is the summation of results obtained from all the different images with identical crack patterns, and n is the total number of images with identical crack patterns. The final accuracy of the model was determined as the average of the accuracy from all images.

3. Results and Discussion

3.1 Quantitative Analysis Through Image Processing Model

There was a total of 54 images obtained randomly from the desiccation tests, which includes 2 images from 10 mm trial set dried at 45°C, 26 from 10 mm specimen dried at 45°C, and 26 from 2 identical 10 mm specimens dried at 105°C. Among those, 8 images were selected randomly to use as training sets for model enhancement and modification work. The average processing time was 1.51s for the model, which means that generally the model used 1.51s to generate all the output from the input raw image. Fig. 3 shows extracted surface crack ratio, average crack width, and their respective accuracy for each image under different test conditions. The accuracy of the model was evaluated by the average accuracy of the whole dataset, except for one image that does not have an identical crack image under different photographic conditions. The final accuracy of the model was computed as 97.24% and 93.85% for surface crack ratio and average crack width respectively.

The determination of surface crack ratio and average crack width is essential in describing the desiccation cracking behaviour of expansive soil as they are highly linked to the shrinkage process during evaporation events. The complexity of crack patterns makes it difficult to be measured on-site, and manual measurement methods are extremely time-consuming with potential crack disruptions that cause measurement errors. Therefore, the use of image processing techniques with high efficiency and accuracy is advantageous to facilitate the crack recognition process.

Fig. 3 shows the surface crack ratio and average crack width distributions with respective accuracies, where D1 to D4 were the drying cycles annotations. For instance, in Fig. 3(a), the data with D1 labels are crack images from onset of cracking to the end of the first drying cycle progressively. Comparing surface crack ratio and average crack width distributions in Fig. 3, it can be observed that the accuracy for average crack width under both testing conditions experienced more fluctuation in general. From the equation for the computation of surface crack ratio and average crack width, as both parameters include dividing crack pixel with denominator, it can be expected that with a high-value denominator comes a low-value result. In this sense, the denominator for surface crack ratio was the background pixel, which was relatively high when compared to crack pixel, leading it to have a comparatively stable range of outputs. Thus, the fluctuation mentioned was mainly due to the rather low-value denominator (skeletonized crack pixel) used to compute average crack width.

From Table 2, it was observed that there are only 2 datasets having accuracy below 70%, while the others fall in the range of 80% - 100%, showing the overall high accuracy achieved by the model. The low accuracy was caused by the circle function that includes circumferential crack lines which formed along the circular shape of the glass container. These crack lines were formed due to the weak bonding between the clay and container at the boundaries which leads to easier crack formation. Such cracks should not be considered in crack quantification as it does not reflect the shrinkage behaviour of the sample. Those datasets with 3 to 5 identical crack images show high accuracy, almost all ranges between 90% to 100%, which presented the reliability and consistency of the model at evaluating bigger datasets. Despite the overall high accuracy, the proposed model is unable to eliminate

the influence of photographic conditions. For instance, the images used as input for the model must be cropped to mould size to help the model in distinguishing information between the inside and outside of the mould. Conversely, the model was able to process images captured under uneven illumination without difficulty and noise removal was done with satisfactory results.

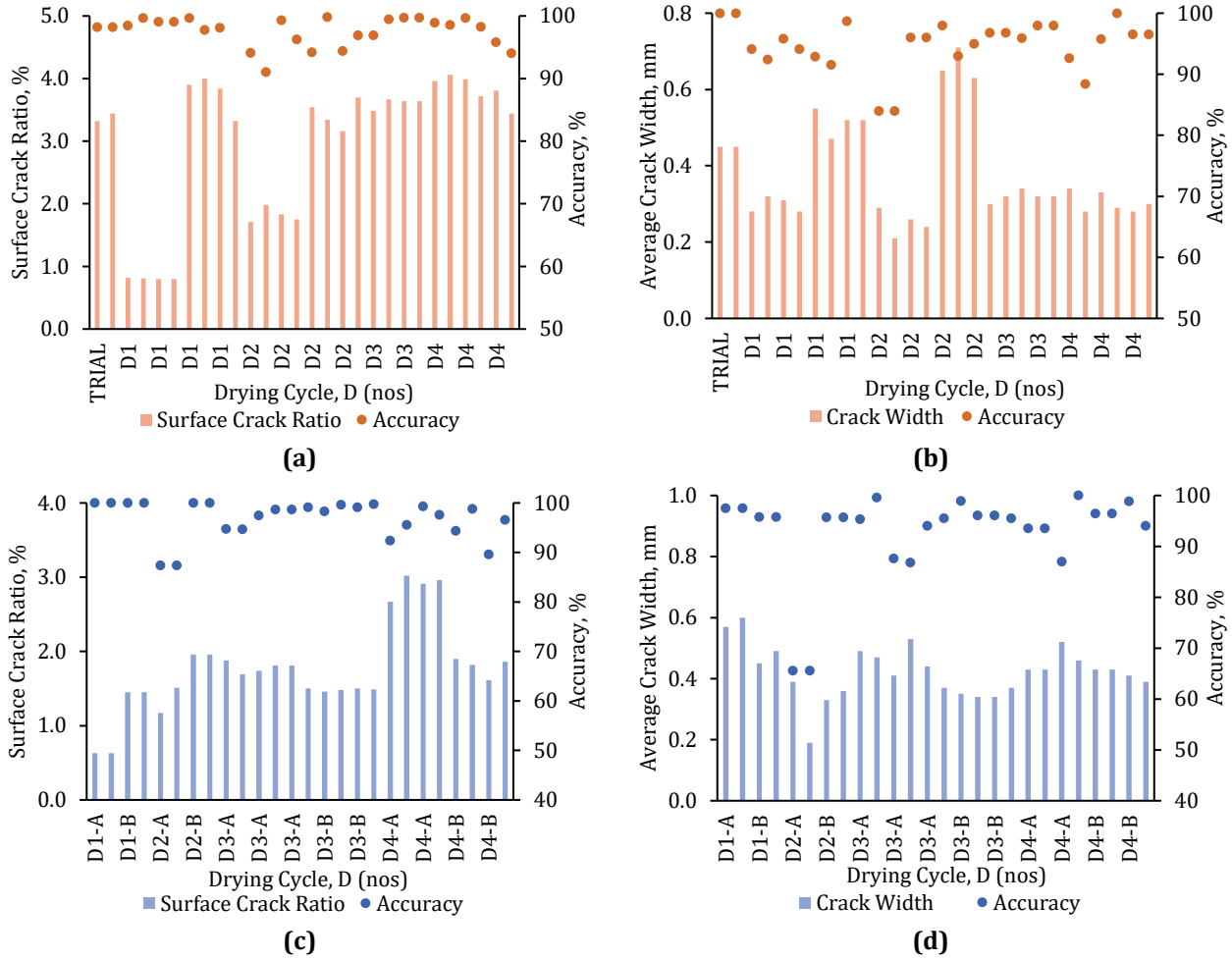

Fig. 3 *Result distribution with respective accuracies (a) Surface crack ratio and (b) average crack width at 45°C; (c) Surface crack ratio and (d) average crack width at 105°C*

Table 2 *Accuracy distribution for each soil parameter*

Accuracy Range	Surface Crack Ratio	Average Crack Width
60% - 70%	0	2
70% - 80%	0	0
80% - 90%	3	6
90% - 100%	50	45

3.2 Surface Crack Ratio and Average Crack Width

In Fig. 4(a) there is a clear increasing trend in the recorded surface crack ratio with increasing drying and wetting cycles for specimens dried at both temperatures. While from Fig. 3(a), the surface crack ratio shows an increment during the drying cycle in the first and second cycles but stabilized in the third and fourth cycles. These results match those observed in earlier studies and the phenomenon was claimed to be caused by the damaged cohesion between the soil particles that eases the generation of cracks [19]. By comparing the 10 mm specimens dried at 45°C and 105°C in Fig. 4(a), it was apparent that the specimen dried at lower temperatures reported a higher surface crack ratio. The possible explanation was that water molecules gained kinetic energy at higher temperatures that facilitated their escape from the formed crack and migration of moisture to the mentioned crack, thus reducing the possibility of crack formation at other parts of the soil surface [20]. In Fig. 3(b), the

Int. Journal of Integrated Engineering Vol. 16 No. 4 (2024) p. 8-15

average crack width in the first and second drying cycles shows increments throughout the cycles, but not in the third and fourth cycles. These observations were not unexpected because the ongoing evaporation leads to increased shrinkage activities during the drying cycles, causing the crack segments to pull in together and increase the crack width between them. In the third and fourth cycles, the cohesion at the sealed crack lines was damaged by previous cracking activities, causing the crack formed at the beginning of the desiccation process to be relatively stable, thus eliminating further changes. From Fig. 4(b), it can be observed that the average crack width in the first and second drying cycles was generally higher than in the third and fourth cycles. This is because as the number of dry-wet cycles increased, the crack segments increased and evened out the shrinkage behaviour throughout the soil surface, thus making each crack have lesser shrinkage activities.

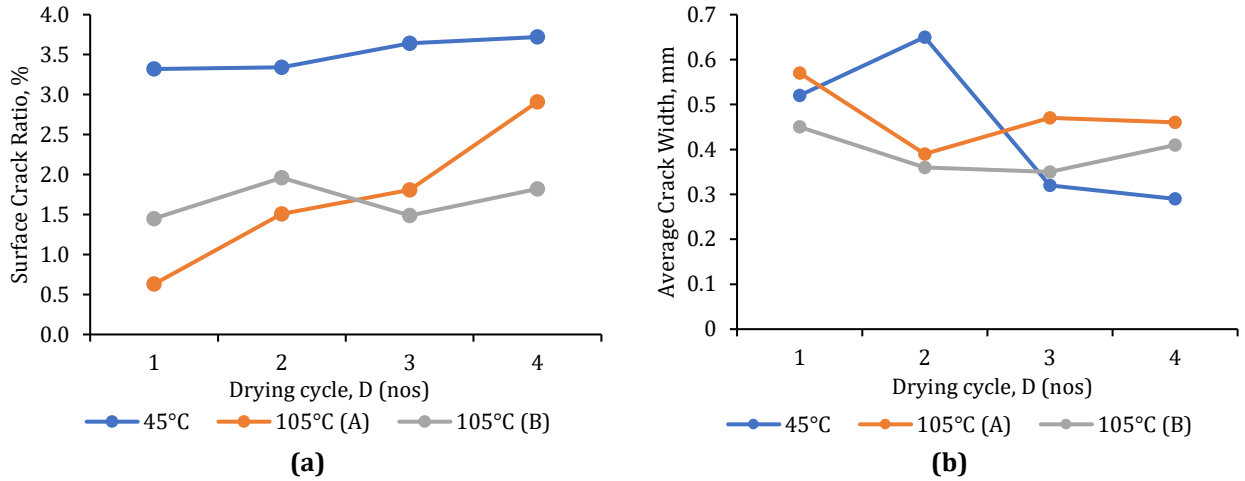

Fig. 4 *Crack parameters at the end of each drying cycle under different drying temperature (a) Surface crack ratio; (b) Average crack width*

4. Conclusion

Machine learning-based image processing model with methods including grey scaling, noise filtering, edge detection, thresholding, and feature extraction was constructed in this study. The proposed image processing model provided an efficient and cost-effective way to quantify crack patterns. Parameters such as surface crack ratio and average crack width were defined to quantify cracks. Desiccation tests were conducted, and crack images were acquired using a digital camera. 54 images were processed with the proposed model and the accuracy for the surface crack ratio and average crack width were 97.24% and 93.85% respectively with 1.51s average processing time per image. The integration of machine learning techniques in the image processing method had been proved a success as the model was able to provide efficient analysis with high accuracy. Despite the downside of needing cropped images to eliminate unnecessary information, the model was able to process images with uneven illumination and noise. Surface crack ratio was found to be increased with increased drying and wetting cycles and decreased drying temperature. Average crack width in the first and second dry-wet cycles was greater than in the third and fourth cycles due to increased crack segments.

Acknowledgement

This research has been carried out under Fundamental Research Grant Scheme project FRGS/1/2022/TK06/UTAR/02/36 provided by Ministry of Higher Education of Malaysia.

Conflict of Interest

Authors declare that there is no conflict of interests regarding the publication of the paper.

Author Contribution

The authors confirm contribution to the paper as follows: ***study conception and design:*** *Ling Hui Yean, Lau See Hung;* ***data collection:*** *Ling Hui Yean, Chong Siaw Yah, Lee Min Lee;* ***analysis and interpretation of results:*** *Ling Hui Yean, Lau See Hung, Yasuo Tanaka;* ***draft manuscript preparation:*** *Ling Hui Yean, Lau See Hung. All authors reviewed the results and approved the final version of the manuscript.*

References

[1] Tang, C. S., Zhu, S., Cheng, Q., Zeng, H., Xu, J. J., Tian, B. G., & Shi, B. (2021). Desiccation cracking of soils: A review of investigation approaches, underlying mechanisms, and influencing factors. Earth-Science Reviews, 216, 103586. https://doi.org/10.1016/j.earscirev.2021.103586

[2] Cheng, Q., Tang, C. S., Xu, D., Zeng, H., & Shi, B. (2021). Water infiltration in a cracked soil considering effect of drying-wetting cycles. Journal of Hydrology, 593, 125640. https://doi.org/10.1016/j.jhydrol.2020.125640

[3] Albrecht, B. A., & Benson, C. H. (2001). Effect of desiccation on compacted natural clays. Journal of Geotechnical and Geoenvironmental Engineering, 127(1), 67-75. https://doi.org/10.1061/(ASCE)1090-0241(2001)127:1(67)

[4] Tang, C. S., Shi, B., Liu, C., Suo, W. B., & Gao, L. (2011). Experimental characterization of shrinkage and desiccation cracking in thin clay layer. Applied Clay Science, 52(1-2), 69-77. https://doi.org/10.1016/j.clay.2011.01.032

[5] Zeng, H., Tang, C. S., Cheng, Q., Lin, L., & Xu, J. J. (2019). Desiccation cracking behavior of soils. Japanese Geotechnical Society Special Publication, 7(2), 90-95. https://doi.org/10.3208/jgssp.v07.013

[6] El Abedine, A. Z., & Robinson, G. H. (1971). A study on cracking in some Vertisols of the Sudan. Geoderma, 5(3), 229-241. https://doi.org/10.1016/0016-7061(71)90012-7

[7] Logsdon, S., Allmaras, R. R., Wu, L., Swan, J. B., & Randall, G. W. (1990). Macroporosity and its relation to saturated hydraulic conductivity under different tillage practices. Soil Science Society of America Journal, 54(4), 1096-1101. https://doi.org/10.2136/sssaj1990.03615995005400040029x

[8] Li, H. D., Tang, C. S., Cheng, Q., Li, S. J., Gong, X. P., & Shi, B. (2019). Tensile strength of clayey soil and the strain analysis based on image processing techniques. Engineering Geology, 253, 137-148. https://doi.org/10.1016/j.enggeo.2019.03.017

[9] Zhao, C., & Koseki, J. (2020). An image-based method for evaluating local deformations of saturated sand in undrained torsional shear tests. Soils and Foundations, 60(3), 608-620. https://doi.org/10.1016/j.sandf.2020.02.012

[10] Shit, P. K., Bhunia, G. S., & Maiti, R. (2015). Soil crack morphology analysis using image processing techniques. Modeling Earth Systems and Environment, 1, 1-7. https://doi.org/10.1007/s40808-015-0036-z

[11] Liu, C., Tang, C. S., Shi, B., & Suo, W. B. (2013). Automatic quantification of crack patterns by image processing. Computers & Geosciences, 57, 77-80. https://doi.org/10.1016/j.cageo.2013.04.008

[12] Al-Jeznawi, D., Sanchez, M., & Al-Taie, A. J. (2021). Using image analysis technique to study the effect of boundary and environment conditions on soil cracking mechanism. Geotechnical and Geological Engineering, 39, 25-36. https://doi.org/10.1007/s10706-020-01376-5

[13] Wang, L. L., Tang, C. S., Shi, B., Cui, Y. J., Zhang, G. Q., & Hilary, I. (2018). Nucleation and propagation mechanisms of soil desiccation cracks. Engineering Geology, 238, 27-35. https://doi.org/10.1016/j.enggeo.2018.03.004

[14] Singh, S. P., Rout, S., & Tiwari, A. (2018). Quantification of desiccation cracks using image analysis technique. International Journal of Geotechnical Engineering, 12(4), 383-388. https://doi.org/10.1080/19386362.2017.1282400

[15] Munawar, H. S., Hammad, A. W., Haddad, A., Soares, C. A. P., & Waller, S. T. (2021). Image-based crack detection methods: A review. Infrastructures, 6(8), 115. https://doi.org/10.3390/infrastructures6080115

[16] Xu, J. J., Zhang, H., Tang, C. S., Cheng, Q., Liu, B., & Shi, B. (2022). Automatic soil desiccation crack recognition using deep learning. Geotechnique, 72(4), 337-349. https://doi.org/10.1680/jgeot.20.P.091

[17] Parente, L., Falvo, E., Castagnetti, C., Grassi, F., Mancini, F., Rossi, P., & Capra, A. (2022). Image-based monitoring of cracks: Effectiveness analysis of an open-source machine learning-assisted procedure. Journal of Imaging, 8(2), 22. https://doi.org/10.3390/jimaging8020022

[18] Han, X. L., Jiang, N. J., Yang, Y. F., Choi, J., Singh, D. N., Beta, P., ..., & Wang, Y. J. (2022). Deep learning based approach for the instance segmentation of clayey soil desiccation cracks. Computers and Geotechnics, 146, 104733. https://doi.org/10.1016/j.compgeo.2022.104733

[19] Tang, C. S., Cui, Y. J., Shi, B., Tang, A. M., & Liu, C. (2011). Desiccation and cracking behaviour of clay layer from slurry state under wetting–drying cycles. Geoderma, 166(1), 111-118. https://doi.org/10.1016/j.geoderma.2011.07.018

[20] Shi, B., Tang, C. S., Wang, B. J., & Jiang, H. T. (2009). Development and mechanism of desiccation cracking of clayey soil under different temperatures. Geological Journal of China Universities, 15(2), 192-198.